

Low anticoagulant heparin targets multiple sites of inflammation, suppresses heparin-induced thrombocytopenia, and inhibits interaction of RAGE with its ligands

Narayanam V. Rao,¹ Brian Argyle,^{1,2} Xiaoyu Xu,² Paul R. Reynolds,³ Jeanine M. Walenga,⁴ Margaret Prechel,⁴ Glenn D. Prestwich,² Robert B. MacArthur,⁵ Bradford B. Walters,⁶ John R. Hoidal,¹ and Thomas P. Kennedy¹

¹Department of Internal Medicine, ²Department of Medicinal Chemistry and Center for Therapeutic Biomaterials, University of Utah Medical Center, Salt Lake City, Utah; ³Department of Physiology and Developmental Biology, Brigham Young University, Provo, Utah; ⁴Hemostasis and Thrombosis Research Laboratories, Loyola University Chicago Stritch School of Medicine, Chicago, Illinois; ⁵Research Pharmacy, Columbia University, New York, New York; and ⁶Research Triangle Institute Health Solutions, Research Triangle Park, North Carolina

Submitted 11 January 2010; accepted in final form 28 March 2010

Rao NV, Argyle B, Xu X, Reynolds PR, Walenga JM, Prechel M, Prestwich GD, MacArthur RB, Walters BB, Hoidal JR, Kennedy TP. Low anticoagulant heparin targets multiple sites of inflammation, suppresses heparin-induced thrombocytopenia, and inhibits interaction of RAGE with its ligands. *Am J Physiol Cell Physiol* 299: C97–C110, 2010. First published April 7, 2010; doi:10.1152/ajpcell.00009.2010.—While heparin has been used almost exclusively as a blood anticoagulant, important literature demonstrates that it also has broad anti-inflammatory activity. Herein, using low anti-coagulant 2-*O*,3-*O*-desulfated heparin (ODSH), we demonstrate that most of the anti-inflammatory pharmacology of heparin is unrelated to anticoagulant activity. ODSH has low affinity for anti-thrombin III, low anti-Xa, and anti-IIa anticoagulant activities and does not activate Hageman factor (factor XII). Unlike heparin, ODSH does not interact with heparin-platelet factor-4 antibodies present in patients with heparin-induced thrombocytopenia and even suppresses platelet activation in the presence of activating concentrations of heparin. Like heparin, ODSH inhibits complement activation, binding to the leukocyte adhesion molecule P-selectin, and the leukocyte cationic granular proteins azurocidin, human leukocyte elastase, and cathepsin G. In addition, ODSH and heparin disrupt Mac-1 (CD11b/CD18)-mediated leukocyte adhesion to the receptor for advanced glycation end products (RAGE) and inhibit ligation of RAGE by its many proinflammatory ligands, including the advanced glycation end-product carboxymethyl lysine-bovine serum albumin, the nuclear protein high mobility group box protein-1 (HMGB-1), and S100 calgranulins. In mice, ODSH is more effective than heparin in reducing selectin-mediated lung metastasis from melanoma and inhibits RAGE-mediated airway inflammation from intratracheal HMGB-1. In humans, 50% inhibitory concentrations of ODSH for these anti-inflammatory activities can be achieved in the blood without anticoagulation. These results demonstrate that the anticoagulant activity of heparin is distinct from its anti-inflammatory actions and indicate that 2-*O* and 3-*O* sulfate groups can be removed to reduce anticoagulant activity of heparin without impairing its anti-inflammatory pharmacology.

receptor for advanced glycation end products; P-selectin; high mobility group box protein-1; S100 calgranulins; human research; translational research

SINCE ITS DISCOVERY A CENTURY AGO (27), heparin has been employed as a blood anticoagulant. However, heparin has also

been long recognized to possess an abundance of anti-inflammatory activities (25). Heparin and low anticoagulant heparin are potent inhibitors of complement activation (14, 46). Heparin can also ameliorate mucus hypersecretion, M₂ muscarinic receptor dysfunction, and airway hyperreactivity from the cationic eosinophil proteins eosinophil cationic protein and major basic protein (4, 13). Heparin and certain low anticoagulant heparin derivatives are potent inhibitors of the adhesion molecules P- and L-selectin, which mediate leukocyte rolling, the initial event governing leukocyte transmigration from the vessel wall into areas of inflammation (45). P- and L-selectin ligation of circulating platelets and monocytes, respectively, by tumor cells also plays an important role in the mediating hypercoagulability and metastasis in patients with cancer (5, 6, 42), explaining the significant improvement in long-term survival when humans with advanced malignancies are treated chronically with low-molecular weight heparins (1, 20, 21, 24). Other anti-inflammatory properties of heparin include potent inhibition of the cationic polymorphonuclear neutrophil (PMN) proteases human leukocyte elastase (HLE) and cathepsin G, both in vitro and in vivo (14). In cells that avidly internalize heparin, such as vascular endothelium, heparin potently inhibits activation and nuclear translocation of NF- κ B (43), one of the major transcriptional inducers of proinflammatory cytokines. Heparin inhibits the β -secretase necessary for processing the amyloid β (A β) precursor protein to the A β peptide (32), and heparin derivatives are neuroprotective in vitro and in vivo against A β toxicity (10). Low anticoagulant heparin analogs have also been shown to bind VEGF and compete with the complexation to cell surface heparan sulfate that is required for VEGF-dependent signaling and angiogenesis (2, 30). Recently, low molecular weight heparin has been reported to inhibit interaction of advanced glycation end-products (AGEs) with receptor for advanced glycation end products (RAGE), blocking the proinflammatory and profibrotic signaling that leads to nephropathy in experimental animal models of diabetic renal failure (29). Thus the spectrum of anti-inflammatory pharmacology demonstrated by heparins is broad and wide ranging. Nevertheless, heparin and low-molecular-weight heparins have not been commonly employed as anti-inflammatory therapies because of the unwanted risk of hemorrhage from anticoagulation.

Address for reprint requests and other correspondence: N. V. Rao, Wintrobe 701, Univ. of Utah Medical Center, 26 North 1900 East, Salt Lake City, UT 84132 (e-mail: Narayanam.Rao@hsc.utah.edu).

We have previously described 2-*O*,3-*O*-desulfated heparin (ODSH), a low anticoagulant heparin derivative produced from cold alkaline hydrolysis of unfractionated heparin, and have characterized its activities as an inhibitor of PMN proteases, complement activation, antigen-induced airways hyperreactivity, reperfusion injury, and NF- κ B activation (14, 43). In the present investigation, we extend our previous observations and demonstrate that while ODSH has low binding affinity for antithrombin III (ATIII), it retains the broad anti-inflammatory pharmacology of the parent heparin, including inhibition of selectins and PMN proteases. Moreover, ODSH appears safer than unfractionated heparin, demonstrating no activation of factor XII. ODSH also does not interact with the heparin-platelet factor-4 (PF4) antibodies that mediate heparin-induced thrombocytopenia (HIT) and even suppresses platelet activation and serotonin release assay (SRA) in the presence of activating concentrations of heparin. Most importantly, ODSH, like heparin, blocks ligation of RAGE with a number of its important ligands, including the AGE-product carboxymethyl lysine-bovine serum albumin (CML-BSA), HMGB-1, and S100 calgranulins. In humans, 50% inhibitory concentrations of ODSH for these anti-inflammatory activities can be achieved in blood without anticoagulation. These results confirm that multiple anti-inflammatory activities of heparin are unrelated to its anticoagulant activity and demonstrate that safe, broadly effective, low anticoagulant anti-inflammatory agents can be developed from this historic molecule.

METHODS

Materials. ODSH was synthesized by Scientific Protein Laboratories (Waukegan, WI) as previously reported (14), using the manufacturer's unfractionated heparin United States Pharmacopeia (USP) as starting material. The resulting batches of material had an average molecular mass of 11.7 ± 0.3 kDa and $90 \pm 0.4\%$ of the HLE inhibitory potency of unfractionated heparin. Fully de-*O*-sulfated heparin, 6-*O* desulfated heparin, carboxyl-reduced heparin, de-*N*-sulfated heparin, heparan sulfate, and low molecular mass heparin (~5 kDa) were purchased from Neoparin (Alameda, CA). Recombinant forms of HMGB-1, Mac-1, P-selectin/Fc chimera, and RAGE/Fc chimera, human azurocidin, polyclonal goat anti-human RAGE, and polyclonal goat anti-human azurocidin were purchased from R&D Systems (Minneapolis, MN). The advanced glycation end-product CML-BSA was from MBL International (Woburn, MA). Human S100b calgranulin was from Calbiochem (San Diego, CA). U937 human monocyte and AMJ2-C11 mouse alveolar macrophage cell lines were from American Type Culture Collection (Manassas, VA). Protein A, horseradish peroxidase (HRP)-conjugated rabbit anti-goat IgG, carbonate-bicarbonate buffer, BSA blocker ($\times 10$), and Inject immunogen EDC conjugation kit with BSA were from Pierce and Warriner (Rockford, IL). Calcein AM, DMEM, EDTA, FBS, HEPES, nonessential amino acids, penicillin/streptomycin/L-glutamine solution, RPMI-1640 without L-glutamine, sodium bicarbonate, and tetramethyl benzidine chromogen (TMB) single solution substrate were from Invitrogen (Carlsbad, CA). High-bind 96-well microplates were from Corning Life Sciences (Corning, NY). All other chemicals not specified were from Sigma-Aldrich (St. Louis, MO).

Cell culture. U937 monocytes were grown in suspension culture at 37°C in humidified 5% CO₂-95% air in RPMI-1640 supplemented with 10% heat-inactivated FBS, 2 mM L-glutamine, 1 mM sodium pyruvate, 0.1 mM MEM nonessential amino acids, 100 U/ml penicillin, and 100 μ g/ml streptomycin. AMJ2C-11 mouse alveolar macrophages were grown at 37°C in humidified 5% CO₂-95% air in DMEM supplemented with 5% FBS, 5 mM HEPES, 0.15 g % sodium

bicarbonate, 2 mM L-glutamine, 100 U/ml penicillin, and 100 μ g/ml streptomycin. Experiments were performed on cells from passages 1–5. B16F10.1 melanoma cells were grown in DMEM, 10% FBS, 100 U/ml penicillin, 100 U/ml streptomycin, 2 mM glutamine, and 1 mM sodium pyruvate.

ODSH/ATIII binding and anticoagulation assays. For studies of ATIII binding, human ATIII was dissolved in PBS and the concentration was determined by measuring absorbance using E_{1%} at 280 nm = 6.5 and a molecular mass of 58 kDa. Heparin and ODSH were dissolved in PBS at a concentration of 50 mg/ml, and further dilutions were made in PBS for the assay. Equilibrium binding titrations of ATIII and ODSH or heparin were performed by monitoring the increase in intrinsic fluorescence of ATIII at excitation 280 nm and emission 340 nm. Fluorescence measurements were performed with a fixed concentration of ATIII (1.72 μ M) and sequential addition of 5–10 μ l of heparin or ODSH solution and corrected for dilution. USP anticoagulant activity and automated amidolytic assays for anti-Xa and anti-IIa activity were performed by BioCascade (Arlington, WI).

SRA for heparin-induced thrombocytopenia. The potential for ODSH (0.78–100 μ g/ml) to activate platelets in the presence of antibodies to PF4 complexes and induce HIT was studied in SRAs. [¹⁴C]SRAs were performed according to methods previously described in detail (34) using sera from three different patients who had demonstrated heparin-PF4 antibodies and who had survived HIT. Activation of radiolabeled platelets, resulting in serotonin release from platelets, was stimulated by addition of 0.1–0.5 U/ml of unfractionated heparin. An SRA-positive experiment with this system results in 20% or greater serotonin release.

Factor XII activation assay. Five microliters of pooled normal human plasma were incubated with 100 μ l of ODSH or heparin in concentrations of 0.1–1,000 μ g/ml in 0.05 M HEPES containing 0.05% TritonX-100 for 5 min at 25°C. Amidolytic activity was determined with 0.5 mM H-D-CHT-Gly-Arg-pNA by following the linear change of optical density (OD) for 30 min at 405 nm (41). The OD obtained at 30 min was plotted against the concentrations of the heparinoids.

Cell surface binding assays. The effect of heparinoids on binding of U937 monocytes to P-selectin or RAGE was studied in high-bind microplates coated with 8 μ g/ml protein A (50 μ l/well) in 0.2 M carbonate-bicarbonate buffer (pH 9.4). Plates were washed with PBS containing 1% BSA (PBS-BSA), and P-selectin-Fc or RAGE-Fc chimera (50 μ l containing 1 μ g) was added to each well and incubated for 2 h at room temperature or overnight at 4°C, respectively. Following incubation, wells were washed twice with PBS-BSA. Fifty microliters of heparinoids (0–1,000 μ g/ml) serially diluted in 20 mM HEPES buffer (containing 125 mM NaCl, 2 mM calcium, and 2 mM magnesium) were added to each well and incubated at room temperature for 15 min. As a negative control, 50 μ l of 10 mM EDTA were added to select wells to prevent cell binding through sequestration of calcium. At the end of the incubation period, 50 μ l of U937 cells (10⁵ cells/well, calcein-labeled according to manufacturer's instructions) were added to each well and plates were incubated an additional 30 min at room temperature. The wells were then washed three times with PBS, and bound cells were lysed by addition of 100 μ l of Tris-Triton X-100 buffer. Fluorescence was measured on a microplate reader using an excitation of 494 nm and emission of 517 nm. The effect of heparinoids on binding of AMJ2C-11 mouse alveolar macrophages to RAGE was studied in a similar fashion.

Solid phase binding assays. Three types of ELISAs were performed, one to study the binding of sulfated polysaccharides to vascular adhesion molecules; one to observe the binding between RAGE and its ligands, including CML-BSA, HMGB-1, and S100b; and competitive ELISAs to study the ability of ODSH to inhibit/compete binding of azurocidin to heparin and the ability of ODSH to inhibit/compete RAGE binding to its ligands.

To study the binding profile of ODSH and other glycosaminoglycans (GAGs) with P-selectin, Mac-1, and RAGE, ODSH or other

GAGs were incubated at 2 $\mu\text{g}/\text{well}$ in 100 μl of PBS for overnight at room temperature. The next day, wells were washed with PBS and blocked with 1% BSA in PBS by incubating at 37°C for 1 h. Next, 100 μl of each adhesion protein, diluted in concentrations from 0.01 to 500 ng/ml, were transferred to each GAG-coated well and incubated at ambient temperature for 3 h. Wells were then washed four times with PBST. To detect bound protein, 100 μl of protein-specific antibody (0.5 $\mu\text{g}/\text{ml}$) were added to each well, the mixture was incubated for 1 h at room temperature, and the wells were washed again four times with PBST. HRP-conjugated secondary antibody (100 μl per well) was added, and the wells were incubated for 1 h at room temperature and then washed once with PBST. A colorimetric reaction was initiated by addition of 100 μl of TMB and terminated after 15 min by addition of 100 μl of 1 N HCl. Absorbance at 450 nm was read using an automated microplate reader. Binding affinity (K_d) was determined from the plot of absorbance values vs. concentrations of adhesion protein.

To confirm RAGE binding to its ligands, polyvinyl 96-well plates were coated with 0.5 $\mu\text{g}/\text{well}$ of specific ligand (CML-BSA, HMGB-1, or S100b calgranulin). Plates were incubated overnight at 4°C and washed three times with PBS-0.05% Tween-20 (PBST). Next, 50 μl of RAGE from the dilution series ranging from 0.001 to ~6 nM were transferred to each respective ligand-coated well and incubated at 37°C for 1 h. Wells were then washed four times with PBST. To detect bound RAGE, 50 μl of anti-RAGE antibody (0.5 $\mu\text{g}/\text{ml}$) were added to each well, the mixture was incubated for 1 h at room temperature, and the wells were washed again four times with PBST. HRP-conjugated secondary antibody (50 μl per well) was added, wells were incubated for 1 h at room temperature, and then washed once with PBST. A colorimetric reaction was initiated by addition of 50 μl of TMB and terminated after 15 min by addition of 50 μl of 1 N HCl. Absorbance at 450 nm was read using an automated microplate reader. K_d was determined from the plot of absorbance values vs. concentrations of RAGE.

For studies of the effect of ODSH or heparin on RAGE binding to its ligands, polyvinyl 96-well plates were coated with specific ligand as described above. Separately, a constant amount of RAGE-Fc chimera (100 μl containing 0.5 $\mu\text{g}/\text{ml}$ in PBST-0.1% BSA) was incubated with an equal volume of serially diluted ODSH or heparin (0.001–1,000 $\mu\text{g}/\text{ml}$ in PBST-BSA) overnight at 4°C. The following day, 50 μl of RAGE-heparinoid mix were transferred to each respective ligand-coated well and incubated at 37°C for 2 h. Wells were then washed four times with PBST. Bound RAGE was detected as described above. Absorbance at 450 nm was plotted against the concentration of ODSH or heparin. The IC_{50} values were obtained using nonlinear regression analysis as described in *Statistical analysis*.

For studies of the effect of ODSH on azurocidin binding to heparin, BSA was conjugated to heparin and purified using a kit from Pierce. Polyvinyl 96-well plates were coated with heparin-BSA by adding 100 μl of a 10 mg/ml solution of conjugate in PBS. Plates were incubated overnight at room temperature and washed twice with PBST. ODSH standards were prepared in PBST. In separate tubes, 50- μl aliquots of ODSH standards were added to 100 μl of human azurocidin (1 $\mu\text{g}/\text{ml}$ in PBST), the volume in each tube was adjusted to 200 μl , and tubes were incubated overnight at 4°C. The following day, 50 μl of each mixture were transferred to the heparin-BSA-coated plate, incubated for 2 h at room temperature, and washed four times with PBST. To detect bound azurocidin, 50 μl of azurocidin antibody (0.5 $\mu\text{g}/\text{ml}$) were added to each well, and plates were incubated for 1 h at room temperature, followed by four washes with PBST. Thereafter, HRP-conjugated secondary antibody, TMB, and 1 N HCl solution were added as described above and absorbance was read at 450 nm using an automated microplate reader. The IC_{50} value was determined from the plot of absorbance values vs. concentrations of ODSH as described for RAGE-ligand assays.

Activity assays of HLE and cathepsin G. The inhibitory activity of heparin and ODSH against HLE and cathepsin G was monitored using

the specific chromogenic substrates Suc-Ala-Ala-Val-*p*NA and Suc-Ala-Ala-Pro-Phe-*p*NA, respectively, according to methods previously described (14).

Melanoma lung metastasis in mice. Lung metastasis from melanoma was studied using protocols previously reported by the Stevenson et al. (42). Animal use and husbandry followed protocols approved by the University of Utah Institutional Animal Care and Use Committee. Confluent B16F10 melanoma cells (70–80%) were harvested by brief exposure to trypsin and washed twice with serum-free medium before injection. Living cells were counted with Trypan blue staining before injection to insure >95% viability. Female C57BL/6J mice ($n = 6$ per group) were injected subcutaneously with 100 μl PBS, 30 mg/kg heparin, or 30 mg/kg ODSH. Thirty minutes later, 5×10^5 B16F10 cells in 200 μl medium were injected intravenously into the lateral tail vein. Mice from each group were injected in alternating order, and cells were resuspended by gently flicking the tube before aspirating the sample for each injection. Twenty-seven days after injection, surviving mice were euthanized. The lungs were removed, perfused intratracheally with 10% buffered formalin, and photographed. Visible tumor foci were counted independently by two different laboratory personnel blinded with regard to treatment groups, with metastasis quantitated by the number of black spots.

HMGB-1-induced lung inflammation in mice. The effect of ODSH on intratracheal HMGB-1 was studied using a protocol recently reported (37). Four-week-old female Balb/C mice were obtained from Jackson Laboratories (Bar Harbor, ME). Animal use and husbandry followed protocols that were approved by the Brigham Young University Institutional Animal Care and Use Committee. Mice ($n = 6$) were assigned to one of three groups: PBS control, HMGB-1 (50 μg), or HMGB-1 (50 μg) + ODSH (100 μg). Mice were anesthetized with 2.5% Avertin, and 25- μl boluses of PBS (or HMGB-1/ODSH as indicated) were nasally inhaled following careful placement on the animal's external nares. The mice were then allowed to recover. Twenty-four hours following nasal inhalation, mice were again anesthetized with 2.5% Avertin and killed and bronchoalveolar lavage fluid was obtained using a 20-gauge surgical catheter intubated into the trachea. A syringe was used to instill and remove four sequential 1.0-ml aliquots of PBS into the lungs, and the resulting fluid was pooled for each animal. Bronchoalveolar lavage fluid was centrifuged at 1,000 g for 10 min at 4°C, and supernatants were assayed for total protein using a BCA total protein kit (ThermoScientific, Rockford, IL) and secreted TNF- α by ELISA using a Quantikine Mouse TNF- α kit (R&D Systems). Pellets were resuspended in 500 μl PBS, and total numbers of cells in the pellets were counted using a hemocytometer. A 250- μl aliquot of the resuspended cell pellets was placed in a cytospin, centrifuged at 1,200 rpm for 5 min, and stained with a modified Wright-Giemsa stain (Diff-Quik; Baxter, McGaw Park, IL). Slides were subjected to a blinded manual differential cell count, and the number of PMNs was determined in each group. Counting was performed in triplicate, and the average was determined.

Autoanalyzer-based assay for plasma ODSH. We developed a rapid and reproducible assay for ODSH in clinical plasma samples based on the residual small binding affinity that ODSH retains for ATIII. In the presence of excesses of both ATIII and coagulation factor Xa, ODSH is able to complex with ATIII and inhibit activity of Xa. The leftover factor Xa cleaves synthetic substrate $\text{CH}_3\text{SO}_2\text{-D-Leu-Gly-Arg-p-nitroaniline}$ to release *p*-nitroaniline (*p*NA). In this system, the quantity of *p*NA released, measured spectrophotometrically at 405 nm, is inversely proportional to the concentration of ODSH present to activate ATIII as a Xa inhibitor, with test plasma samples compared with a standard curve performed with auto concentrations of ODSH. Using this principle, we developed an autoanalyzer based assay using the commercially available Stachrom heparin kit (Diagnostica Stago, Asnieres, France) used to assay heparin in clinical plasma samples based on the anti-Xa method. The assay was validated at both 37° and 25°C for measuring ODSH in physiologic buffers, fresh citrated plasma, and citrated plasma exposed to freeze-thaw conditions and

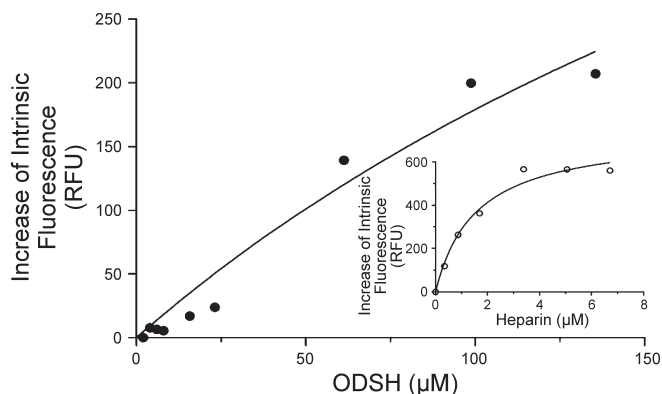


Fig. 1. 2-*O*,3-*O*-desulfated heparin (ODSH) has low binding affinity for antithrombin-III. Binding of antithrombin III to ODSH or heparin (*inset*) was studied as outlined in METHODS. RFU, relative fluorescence units.

proved accurate for measurement of plasma ODSH within a relevant concentration range of 10 to 200 µg ODSH/ml. All clinical assays were performed under Good Laboratory Practices conditions by BioCascade, (Arlington, WI). Assay results were used to determine pharmacokinetic parameters of intravenous ODSH using WinNonlin (Version 4.1).

Phase I intravenous ODSH administration to normal human volunteers. ODSH was studied in normal human volunteers under Investigational New Drug application 71,356, using three protocols. Clinical studies of ODSH were performed in accordance with clinical research guidelines established in U.S. 21 Code of Federal Regulation Part 312.20, the principles enunciated in the Declaration of Helsinki IV (Hong Kong, September, 1989) and the International Conference on Harmonisation guideline regarding Good Clinical Practices, and were registered with clinicaltrials.gov. Protocols were approved by independent Institutional Review Boards, and written informed consent was obtained from each subject in a language in which the subject was fluent. Volunteers were between the ages of 18 and 60 yr of age, had normal values for hemoglobin and coagulation function, no evidence of liver or renal dysfunction, no recent episodes of gastrointestinal bleeding or surgical procedures, no history of heparin-induced thrombocytopenia, and were not pregnant.

In the first study, 39 subjects (35 males and 4 females) were randomized to escalating intravenous bolus infusions of ODSH or saline placebo over 15 min at doses of 4 mg/kg (4 males and 4 females randomized 3:1 within gender to ODSH or placebo), 8 mg/kg (8 males randomized 3:1 ODSH:placebo), 12 mg/kg (8 males randomized 3:1 ODSH:placebo), 16 mg/kg (8 males randomized 3:1 ODSH:placebo), and 20 mg/kg (5 males randomized 4:1 ODSH:placebo). In an additional two male subjects, unfractionated heparin was administered in a bolus dose of 80 U/kg (0.571 mg/kg) for comparison. Blood was obtained before and at serial times for up to 24 h after bolus drug infusion to monitor serum chemistries, complete blood count, partial thromboplastin (PT), activated partial thromboplastin time (aPTT), activated clotting time, and ODSH concentration.

In the second study, 24 male subjects were randomized to ODSH or placebo administered by intravenous bolus followed by constant infusion of drug or placebo for 12 h. Doses included 8 mg/kg bolus with infusion of 24 mg·kg⁻¹·12 h⁻¹ (6 subjects randomized 4:2 ODSH:placebo), 8 mg/kg bolus with infusion of 32 mg·kg⁻¹·12 h⁻¹ (8 subjects randomized 6:2 ODSH:placebo), 8 mg/kg bolus with infusion of 47.5 mg·kg⁻¹·12 h⁻¹ (2 subjects randomized 2:0 ODSH:placebo), and 16 mg/kg bolus with infusion of 32 mg·kg⁻¹·12 h⁻¹ (8 subjects randomized 6:2 ODSH:placebo). Blood was obtained before and at serial times for up to 24 h after bolus drug infusion to monitor serum chemistries, complete blood count, PT, aPTT, and ODSH concentration.

In the third study, 6 subjects (4 males and 2 females) were administered ODSH administered in open-label fashion as a bolus of 8 mg/kg followed by an initial infusion of 0.58 mg·kg⁻¹·h⁻¹. Thereafter, the infusion rate of ODSH was adjusted to maintain an aPTT between 40 and 45 s for a total drug infusion time of 72 h. Blood was obtained before and at serial times for up to 17 days after bolus drug infusion to monitor serum chemistries, complete blood count, PT, aPTT, and ODSH concentration.

Statistical analysis. Results are expressed as means ± SE. In vitro data from saturation binding experiments were analyzed using the GraphPad Prism program (GraphPad Software, San Diego, CA) to obtain K_d values. In vitro data from inhibitory experiments were

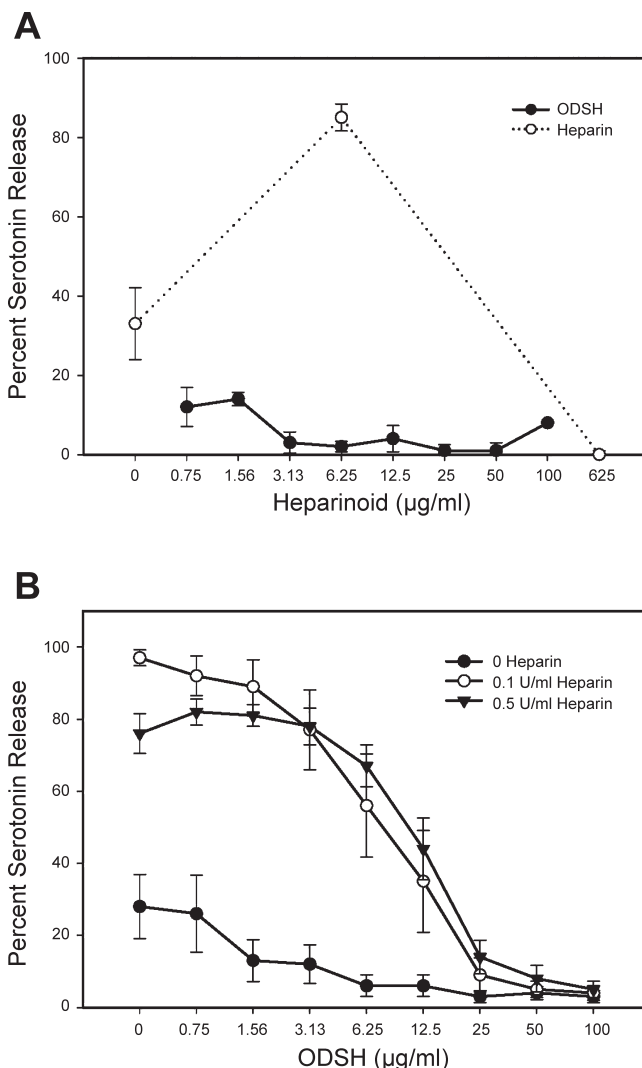


Fig. 2. ODSH does not trigger platelet activation in the heparin-induced thrombocytopenia (HIT) serotonin release assay and suppresses serotonin release by heparin. A: ODSH does not stimulate serotonin release. Donor platelets from normal subjects were loaded with [¹⁴C]serotonin and incubated with serum from 3 individual subjects with heparin-platelet factor 4 (PF4) antibodies. Activation of platelet serotonin release was stimulated by addition of low concentrations of unfractionated heparin as a positive control and was compared with levels of serotonin release in the presence of escalating concentrations of ODSH. An SRA-positive experiment with this system results in 20% or greater serotonin release. Note that high concentrations of heparin suppress platelet activation and serotonin release. B: ODSH suppresses serotonin release induced by heparin. When added in concentrations ≥25 µg/ml, ODSH suppressed serotonin release stimulated by either 0.1 (antithrombotic) or 0.5 U/ml (anticoagulant) concentrations of heparin.

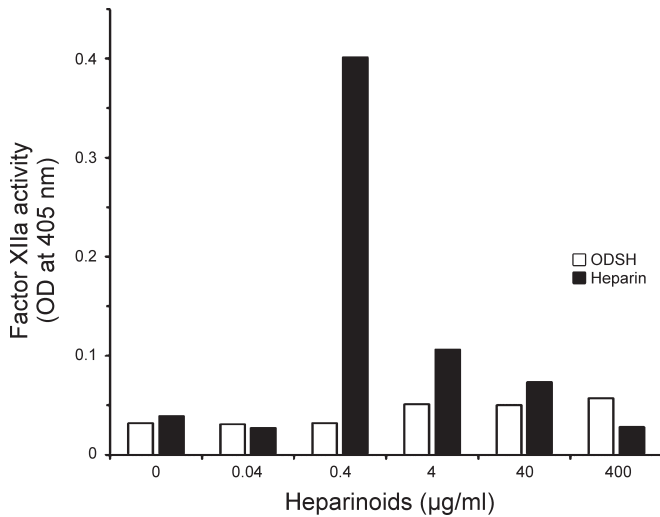


Fig. 3. ODSH does not activate Hageman factor (factor XII). Pooled human plasma was incubated with heparin or ODSH and amidolytic activity was determined using the substrate D-cyclohydroxytyrosyl-Gly-Arg-p-NA. Unfractionated heparin provides typical activation at a concentration of 0.4 µg/ml but suppresses at higher concentrations. In contrast, ODSH fails to activate factor XII at any concentration. OD, optical density.

analyzed using SoftMax Pro (Molecular Devices) software by fitting the data in a 4-parameter logistic nonlinear regression equation to obtain the IC₅₀ values. In vivo experiments with multiple groups or treatments were analyzed using a one-way ANOVA followed by Student-Newman-Keuls post hoc test to probe for group differences. In experiments with two groups, the paired Student's *t*-test was used to assess difference. Significance was assigned at *P* < 0.05.

RESULTS

ODSH has low affinity for ATIII and reduced anticoagulant activity. We previously have shown that ODSH has low anticoagulant activity (14, 43). We further evaluated the anticoagulant property of ODSH by testing its affinity for ATIII. As shown in Fig. 1, ODSH had low affinity for ATIII (*K_d* = 339 µM or 4 mg/ml vs. 1.56 µM or 22 µg/ml for heparin) and is consistent with its low anticoagulant activity as judged by

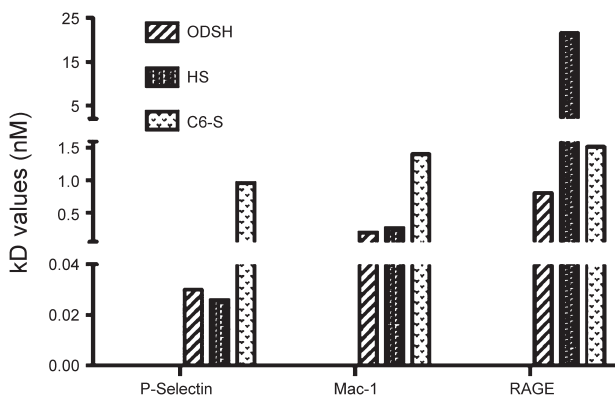


Fig. 4. ODSH and other GAGs bind to vascular adhesion proteins. ODSH, heparan sulfate (HS), and chondroitin 6-sulfate (C6-S) were studied to determine binding affinity of these GAGs for P-selectin, Mac-1, and receptor for advanced glycation end products (RAGE). Binding affinity (*K_d*) values displayed are determined from individual plots shown in Supplemental Fig. 1. Compared with HS or C6-S, ODSH has greater affinity for all 3 adhesion proteins.

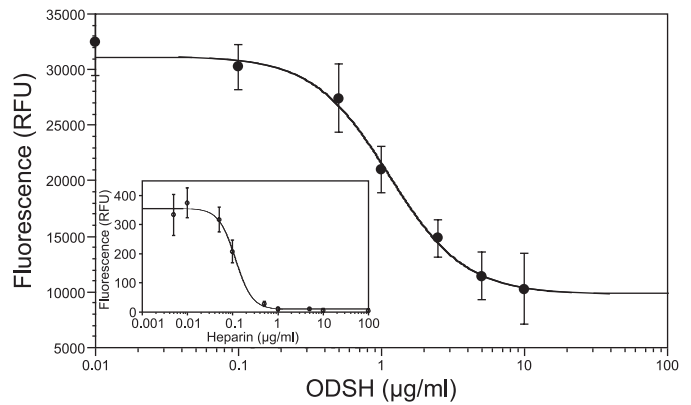


Fig. 5. ODSH and heparin inhibit P-selectin-mediated cellular adhesion. Concentration-dependent interaction between PSGL-1-mediated U937 cells binding to immobilized P-selectin-Fc chimera was studied as outlined in METHODS. Each data point represents means ± SE of 8 values obtained in 2 experiments. Binding is expressed as RFU. IC₅₀ for P-selectin inhibition is 1.1 with ODSH (●) and 0.11 µg/ml for heparin (○).

anti-Xa and anti-IIa activities. Seven serially produced batches of ODSH demonstrated consistently reduced USP (7 ± 0.3 U of anticoagulant activity/mg), anti-Xa (1.9 ± 0.1 U/mg), and anti-IIa (1.2 ± 0.1 U/mg) activities, compared with those of heparin (165–190 U/mg activity for all 3 assays).

ODSH does not trigger platelet activation in vitro of HIT and suppresses HIT in the presence of heparin. A complication of heparin therapy is HIT, which occurs in subjects who produce an activating antibody to the heparin-PF4 complex on the platelet cell surface, resulting in >50% fall in circulating platelet levels, together with greatly increased risk of venous and arterial thromboembolism (44). We therefore determined whether ODSH shared this property with heparin. Unlike heparin, ODSH failed to trigger platelet activation in the presence of HIT antibodies, measured in the SRA over a wide range of concentrations (Fig. 2A).

High concentrations of heparin (>100 µg/ml) have been long known to suppress serotonin release in the presence of an antibody to the heparin-PF4 complex (Fig. 2A). We therefore

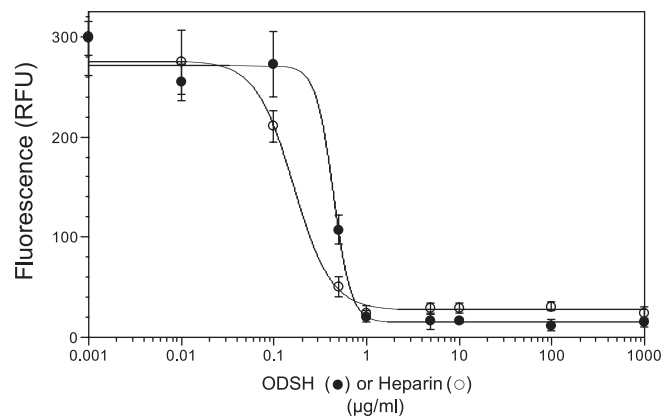


Fig. 6. ODSH and heparin inhibit binding of alveolar macrophages to RAGE. Concentration-dependent inhibition of interaction between Mac-1-mediated AMJ2C-11 alveolar macrophage binding to immobilized RAGE-Fc chimera was studied as described in METHODS. Data points in each figure represent the average value of quadruplicate wells for each concentration of polysaccharide. ODSH (●) and heparin (○) inhibiting binding of alveolar macrophages to RAGE with IC₅₀ values of 0.4 and 0.2 µg/ml, respectively.

tested ODSH added along with heparin in the SRA. When present in concentrations as low as 25 $\mu\text{g/ml}$, ODSH completely suppressed serotonin release stimulated by 0.1 or 0.5 U/ml heparin (Fig. 2B), suggesting that ODSH can competitively inhibit antibody-induced platelet activation in the presence of both antithrombotic (0.1 U/ml) and anticoagulant (0.5 U/ml) concentrations of heparin.

ODSH does not activate factor XII. Negatively charged heparinoids can activate factor XII and initiate coagulation via factor XIIa, producing an inflammatory response mediated by the kallikrein-kinin and complement cascades (38). Therefore, we performed an in vitro assay to test the ability of ODSH to activate factor XII compared with heparin (Fig. 3). Heparin increased the amidolytic activity to maximum at 0.4 $\mu\text{g/ml}$, but higher concentrations of heparin inhibited the reaction. In contrast, ODSH showed low amidolytic activity that was not different from that of control. As a result, ODSH does not stimulate the formation of kallikrein, which can generate active C3 and C5 of complement components and activate β -factor XIIa to produce active C1r and C1s.

ODSH and other GAGs bind to vascular adhesion proteins. We studied the binding affinity of three adhesion proteins (P-selectin, Mac-1, and RAGE) to ODSH and compared their affinity to heparan sulfate (HS) and chondroitin 6-sulfate (C6-S). The data, expressed as K_d of each protein for a GAG, are shown in Fig. 4, with displays of plots for each GAG and vascular adhesion protein shown in Supplemental Fig. 1 (supplemental data for this article are available online at the *Am J Physiol Cell Physiol* website). Results suggest that the three proteins have greater affinity for ODSH and HS except in the case of RAGE, which showed a K_d for HS of 21.5 nM. Although the proteins showed less affinity for C6-S compared with ODSH, the K_d values with all three were in the nanomolar range (~ 1 –1.5 nM), indicating that C6-S can bind as strongly to P-selectin, Mac-1, and RAGE as ODSH.

ODSH and heparin inhibit P-selectin glycoprotein ligand-1-mediated U937 cell binding to P-selectin. Complement activation often leads to leukocyte recruitment. The first step in leukocyte recruitment involves interaction between P-selectin on endothelium and its natural ligand, P-selectin glycoprotein ligand-1 (PSGL-1), which is expressed on the surface of leukocytes (28). Heparin can act as a ligand for P-selectin and disrupt the binding of P-selectin to PSGL-1 (22, 45). We therefore assessed the effect of ODSH on adhesion of PSGL-1 expressing U937 cells to P-selectin. Both heparin and ODSH

prevented adhesion between P-selectin and U937 cells with IC_{50} values of 0.11 and 1.1 $\mu\text{g/ml}$, respectively (Fig. 5). A 10-fold higher ODSH concentration (10 $\mu\text{g/ml}$) prevented 90% of the binding.

ODSH and heparin inhibit Mac-1-mediated binding of inflammatory cells to RAGE. In a subsequent step of leukocyte infiltration, cells loosely bound to P-selectin firmly attach to endothelium through interaction of the β_2 -integrin Mac-1 (CD11b/CD18), present on the leukocyte surface, with intercellular adhesion molecule-1 (ICAM-1) on endothelium. In vivo studies (8) have indicated the existence of ICAM-1-independent inflammatory cell recruitment based on Mac-1-mediated attachment to RAGE. Both Mac-1 and RAGE bind heparin (11, 17). We therefore tested whether ODSH and heparin might interfere with Mac-1 mediated binding of AMJ2-C11 mouse alveolar macrophages to immobilized RAGE. Both ODSH and heparin inhibited binding of alveolar macrophages to RAGE with IC_{50} values of 0.4 $\mu\text{g/ml}$ for ODSH and 0.2 $\mu\text{g/ml}$ for heparin (Fig. 6).

In chronic inflammatory conditions, monocytes can transform into tissue macrophages. We therefore evaluated the ability of ODSH to disrupt Mac-1-mediated binding of U937 monocytes to immobilized RAGE. ODSH and heparin effectively inhibited the binding of U937 cells to RAGE with IC_{50} values of 0.11 and 0.10 $\mu\text{g/ml}$, respectively (Table 1). The parent molecule for ODSH, unfractionated porcine heparin, is heterogeneous with regard to sulfation, charge, and size (25). To evaluate structure-activity relationships, we tested the inhibitory potency of heparin and modified heparins on U937 cells adherence to RAGE (Table 1). Whereas heparin, ODSH, and 6-*O* desulfated heparin inhibited monocyte-RAGE interaction with an IC_{50} of ~ 0.1 $\mu\text{g/ml}$, completely *O*-desulfated heparin showed very poor inhibitory potency (IC_{50} for de-*O* sulfated heparin = 14.75 $\mu\text{g/ml}$). Desulfation at *N*-position of glucosamine of heparin also showed significantly reduced inhibitory potency (IC_{50} for de-*N* sulfated heparin = 0.48 $\mu\text{g/ml}$). This suggests that Mac-1-mediated U937 cell binding to RAGE requires at least one *O*-sulfate in conjunction with *N*-sulfation for maximal inhibitory potency. Heparan sulfate, present on endothelium, showed a 10-fold reduction in inhibitory potency (IC_{50} = 1.12 $\mu\text{g/ml}$) in attenuating the Mac-1 and RAGE interaction. Low molecular mass heparin (~ 5 kDa) demonstrated an inhibitory potency fivefold less (IC_{50} = 0.48 $\mu\text{g/ml}$), and carboxyl-reduced heparin was twofold less active (IC_{50} for carboxyl-reduced heparin = 0.23 $\mu\text{g/ml}$) compared

Table 1. Effect of heparinoids on Mac-1-mediated U937 cell binding to RAGE

Compound	Uronic Acid		Glucosamine		IC_{50}		Relative Affinity
	2	3	6	2-N	$\mu\text{g/ml}$	r^2	
Heparin	●	●	●	●	0.096	0.999	1.0
ODSH	○	○	●	●	0.11	0.992	0.87
6- <i>O</i> -desulfated	●	●	○	●	0.11	0.997	0.87
De- <i>O</i> -sulfated	○	○	○	●	14.75	0.987	0.01
De- <i>N</i> -sulfated	●	●	●	○	0.48	0.998	0.20
Heparin low molecular weight (5,000)					0.48	0.950	0.20
Heparan sulfate					1.12	0.984	0.09
Carboxyl reduced					0.23	0.996	0.42

Uronic acid is either iduronic acid or glucuronic acid. Relative affinity is expressed as the ratio between IC_{50} of heparin and IC_{50} of modified heparin. Numbers represent the *O*-sulfated positions in uronic and glucosamine (●) and modifications (desulfation; ○). ODSH, 2-*O*,3-*O*-desulfated heparin; RAGE, receptor for advanced glycation end products.

with partially *O*-desulfated heparin or heparin. These observations indicate that attenuation of Mac-1-mediated U937 cell binding to RAGE requires sulfation of at least one of three possible *O*-positions, that *N*-sulfation is essential for full inhibitory potency of partially *O*-sulfated heparins, and that both larger size and intact carboxyl groups are also important for full activity of RAGE binding to heparins.

ODSH and heparin interfere with the binding and biological activities of leukocyte granular proteins. When leukocytes attach to vascular endothelium, Mac-1-mediated adherence results in the release of the cationic protein azurocidin specifically stored in secretory vesicles. Azurocidin is a homologue of HLE but with a catalytic site that is mutated and dysfunctional (15). Released azurocidin binds to the heparan sulfate-rich glycocalyx on endothelial cells and produces an increase in vascular permeability, thereby facilitating egress of leukocytes to sites of inflammation (15). We speculated ODSH and heparin might compete with endothelial cell heparan sulfate for azurocidin binding. ODSH inhibited the binding of azurocidin to heparin-BSA-coated wells with an IC_{50} of 4.1 $\mu\text{g/ml}$ (Fig. 7), compared with an IC_{50} of 2.7 $\mu\text{g/ml}$ for heparin studied under identical conditions.

Leukocytes that extravasate to sites of inflammation or injury discharge their primary granular proteins into the extracellular environment, producing proteolytic cell and tissue destruction (47) and also playing an important regulatory role in noninfectious inflammatory processes by degrading adhesion molecules, activating specific receptors, and modulating the levels of cytokines (33). Therefore, we evaluated the inhibitory capacity of ODSH and heparin on HLE (Fig. 8A) and cathepsin G (Fig. 8B) activities. ODSH and heparin decreased >90% of the enzymatic activity of both proteins, with IC_{50} values for HLE and cathepsin G of 0.22 and 0.28 $\mu\text{g/ml}$, respectively, for ODSH, compared with 0.21 and 0.28 $\mu\text{g/ml}$, respectively, for heparin (Table 2). The calculated inhibitory constants (K_i ; Ref. 9) were ~ 10 – 15 nM for both the enzymes, suggesting that ODSH is a potent inhibitor of HLE and cathepsin G. We further processed data for HLE or cathepsin G binding stoichiometry with ODSH. Results also indicate that 2.5 mol of HLE and 1.81 mol of cathepsin G bind per mol of

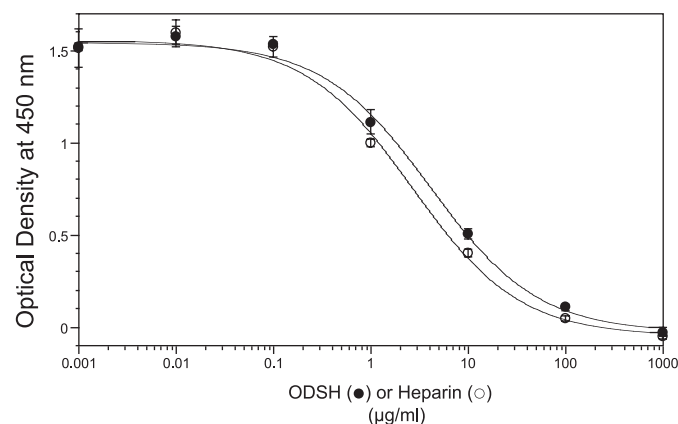


Fig. 7. ODSH and heparin inhibit binding of azurocidin to immobilized heparin. Concentration-dependent binding of azurocidin to immobilized glycosaminoglycans (heparin-BSA) was studied as described in METHODS. Data are means of triplicate wells for each concentration of polysaccharide in a typical experiment. IC_{50} for inhibition of azurocidin binding was 4.1 $\mu\text{g/ml}$ for ODSH (●) and 2.7 $\mu\text{g/ml}$ for heparin (○).

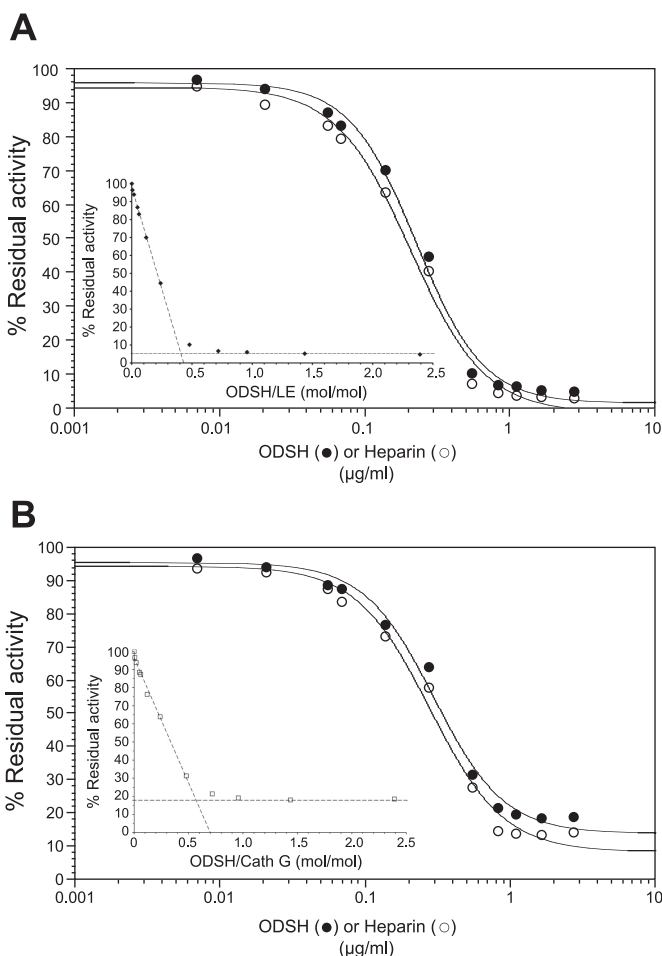


Fig. 8. ODSH and heparin inhibit activity of cationic PMN proteases. *A*: ODSH and heparin inhibit human leukocyte elastase (HLE). Concentration-dependent inhibition of HLE by ODSH was tested using the synthetic chromogenic substrate Suc-Ala-Ala-Val-*p*NA. Change in OD in the absence of inhibitor is considered as 100% to calculate the percent residual activity. *Inset*: graph for the determination ODSH/LE binding stoichiometry. ODSH (●) and heparin (○) inhibited HLE activity with IC_{50} values of 0.22 and 0.21 $\mu\text{g/ml}$, respectively. *B*: ODSH and heparin inhibit leukocyte cathepsin G. Concentration-dependent inhibition of leukocyte cathepsin G by ODSH was tested using the synthetic chromogenic substrate Suc-Ala-Ala-Pro-Phe-*p*NA. OD change in the absence of inhibitor is considered as 100% to calculate the percent residual activity. *Inset*: graph for the determination ODSH/Cathepsin G binding. ODSH (●) and heparin (○) inhibited cathepsin G activity with IC_{50} values of 0.30 and 0.28 $\mu\text{g/ml}$, respectively.

ODSH. These experiments illustrate that removal of 2-*O* and 3-*O* sulfates in iduronic acid and glucosamine, respectively, has no effect on inhibition of HLE and cathepsin G.

ODSH and heparin inhibit interaction of RAGE with its disparate ligands. RAGE functions as a pattern recognition receptor, interacting with multiple structurally unrelated ligands other than Mac-1, including HMGB-1 or amphoterin (19) and members of the S100/calgranulin protein family (18), thereby serving as a progression factor to amplify inflammatory responses (40). Because heparin has been used to remove radioactive ligands bound to RAGE (39), we reasoned that ODSH and heparin might interfere with the binding of RAGE to its heterogeneous ligands.

To study the effect of ODSH and heparin on interaction between RAGE and AGE, we selected CML-BSA, which is the

Table 2. Heparin and ODSH inhibit leukocyte proteases

Parameter	Heparinoid	
	ODSH	Heparin
Elastase		
IC ₅₀ , µg/ml	0.22	0.21
IC ₅₀ , nM	19.5	14.9
K _i , nM	15.1	11.4
Inhibitor/enzyme, mol/mol	0.4	0.32
Enzyme/inhibitor, mol/mol	2.5	3.12
Cathepsin G		
IC ₅₀ , µg/ml	0.30	0.28
IC ₅₀ , nM	25.7	20.2
K _i , nM	15.2	11.9
Inhibitor/enzyme, mol/mol	0.55	0.41
Enzyme/inhibitor, mol/mol	1.81	2.45

Inhibitory constant (K_i) was calculated using Cheng-Prusoff equation from Ref. 9. Inhibitor/enzyme is the x coordinate value of the intersection of linear portion of the plot and horizontal line of minimum activity when the results are plotted as %residual activity vs. the inhibitor-to-enzyme molar ratio; x value is inhibitor-to-enzyme binding ratio or equivalence point. Enzyme/inhibitor is the reciprocal of equivalence point.

AGE product found most abundantly *in vivo*. RAGE bound to immobilized CML-BSA in a dose-dependent manner with a K_d of 0.43 nM (Fig. 9A, *inset*). ODSH and heparin inhibited the RAGE-CML-BSA interaction with IC₅₀ values of 8.6 and 0.4 µg/ml, respectively (Fig. 9A).

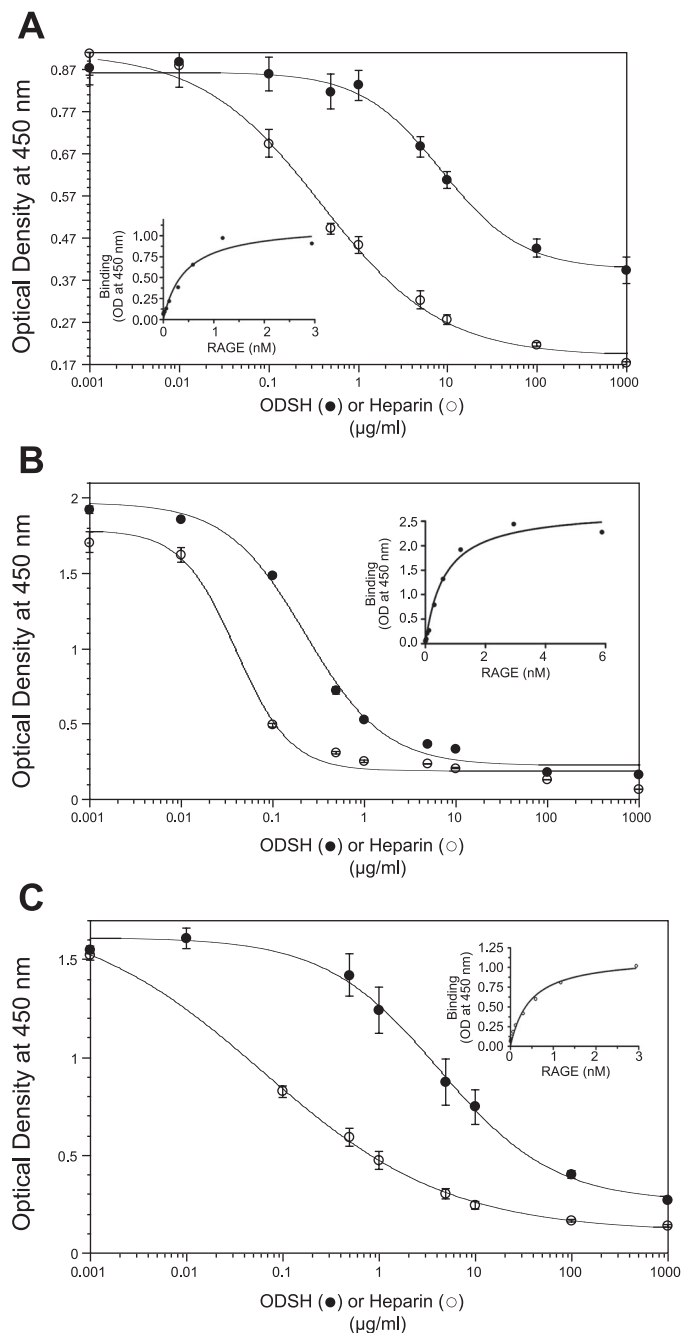
HMGB-1 was also originally isolated as a heparin binding protein (36) and has a heparin-binding consensus sequence present in its the amino terminus (7). RAGE bound to immobilized HMGB-1 in a saturable fashion (Fig. 9B, *inset*) with a K_d of 0.64 nM. ODSH and heparin blocked RAGE-HMGB-1 interaction with IC₅₀ values of 0.23 and 0.04 µg/ml, respectively (Fig. 9B).

S100/calgranulins are RAGE ligands secreted by leukocytes. RAGE engaged immobilized S100b in a dose-dependent manner, with a K_d of 0.45 nM (Fig. 9C, *inset*). ODSH and heparin blocked RAGE binding to S100b with IC₅₀ values of 4.23 and 0.06 µg/ml (Fig. 9C).

ODSH reduces melanoma lung metastasis in mice. Heparins have been previously shown to inhibit metastatic tumor spread

Fig. 9. ODSH and heparin inhibit interaction of RAGE with its disparate ligands. **A:** ODSH and heparin inhibit binding of carboxymethyl lysine-bovine serum albumin (CML-BSA) to RAGE. CML-BSA binding to RAGE-Fc chimera was studied using ELISA techniques described in METHODS. RAGE bound to immobilized CML-BSA in a dose-dependent manner with a K_d of 0.43 nM (*inset*). Data are means of triplicate wells for each concentration of polysaccharide in a typical experiment. ODSH (●) and heparin (○) inhibit CML-BSA binding to RAGE with IC₅₀ values of 8.6 and 0.4 µg/ml, respectively. **B:** ODSH and heparin inhibit binding of HMGB-1 to RAGE. Human HMGB-1 binding to RAGE-Fc chimera was studied using ELISA techniques described in METHODS. RAGE bound to immobilized human HMGB-1 in a saturable fashion (*inset*) with a K_d of 0.64 nM. Data are means of quadruplicate wells for each concentration of polysaccharide in a typical experiment. ODSH (●) and heparin (○) inhibit binding of human high mobility box group protein-1 (HMGB-1) to RAGE with IC₅₀ values of 0.23 and 0.04 µg/ml, respectively. **C:** ODSH and heparin inhibit binding of S100b calgranulin to RAGE. Human S100b binding to RAGE-Fc chimera was studied using ELISA techniques described in METHODS. RAGE engaged immobilized S100b in a dose-dependent manner, with a K_d of 0.45 nM. Data are means of quadruplicate wells for each concentration of polysaccharide in a typical experiment. ODSH (●) and (○) inhibit binding of human S100b binding to RAGE with an IC₅₀ values of 4.23 and 0.06 µg/ml, respectively.

by blocking P- and L-selectin-mediated platelet and monocyte attachment to circulating tumor cells, which cloaks and protects metastasizing cells as they course through the circulation (6, 7, 42). To determine if it can functionally block selectins *in vivo*, we studied the ability of ODSH to prevent lung metastasis from intravenously injected B16 melanoma cells. A single subcutaneous dose of heparin significantly decreased lung metastasis at 28 days after melanoma cell injection, but the same dose of ODSH (30 mg/kg) provided a substantially greater reduction in numbers of lung metastases than did heparin (Fig. 10A). Corresponding lung histology sections are shown in Fig. 10B. ODSH also significantly improved 28-day survival. In contrast to 70% mortality in mice treated with PBS, ~70% of mice treated with ODSH survived (Fig. 10C).



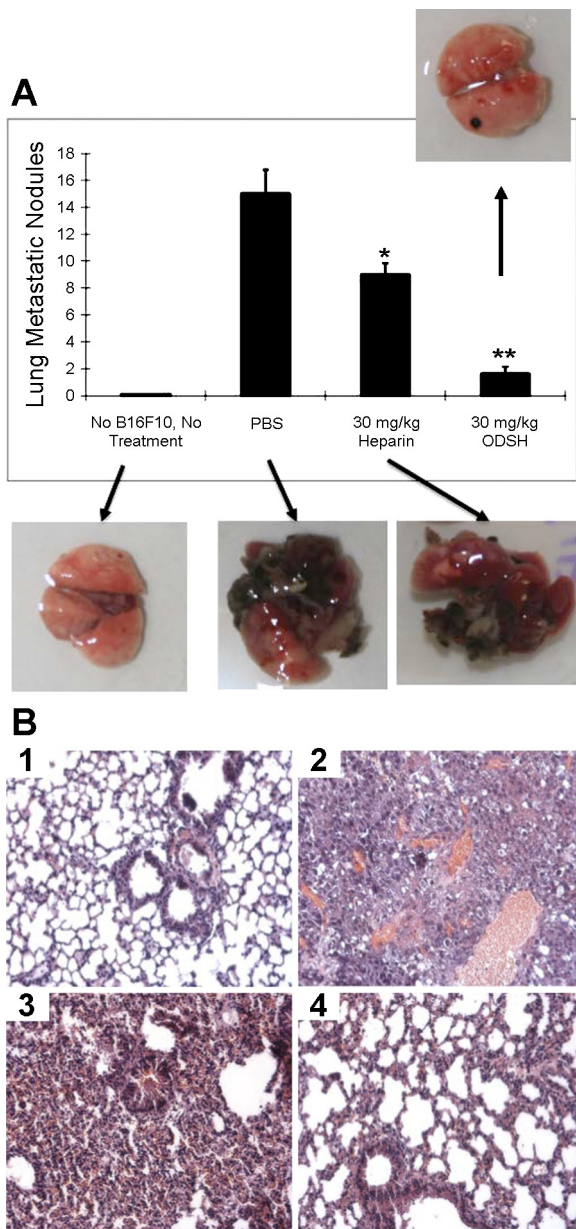


Table 3. ODSH inhibits inflammation from intratracheal HMGB-1 in mice

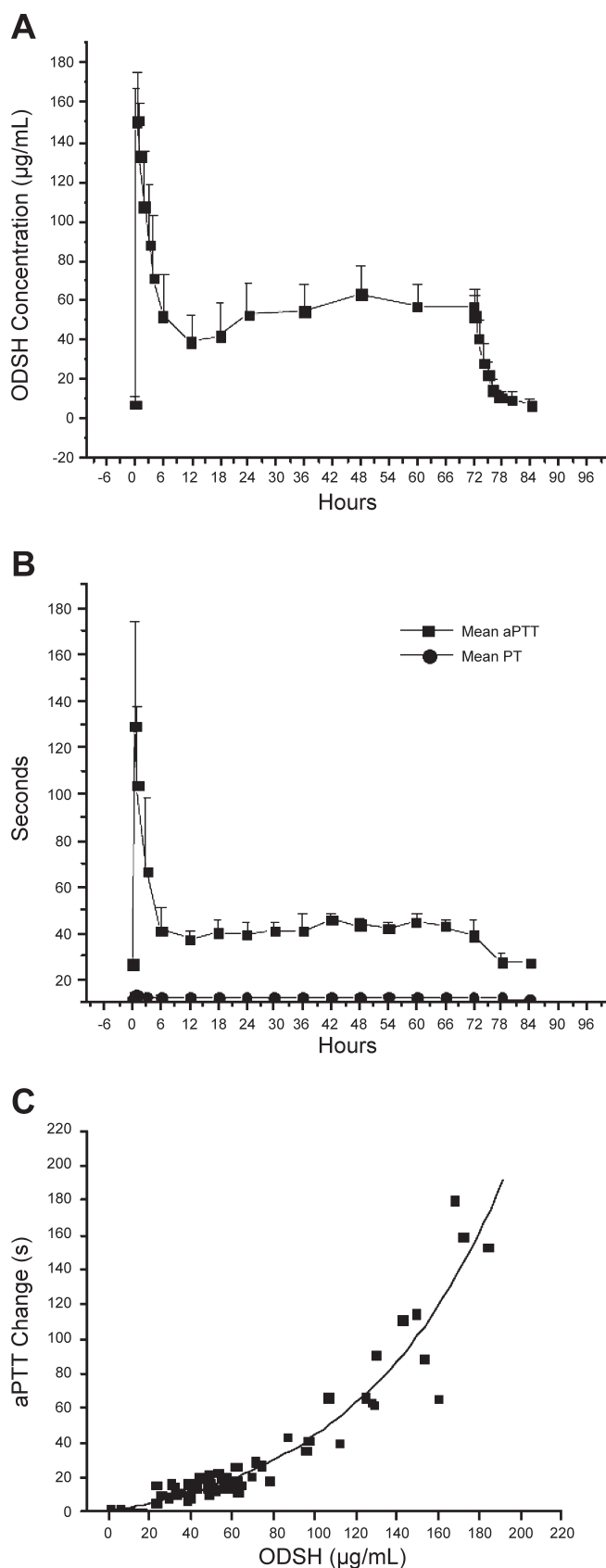
	Group 1 (PBS)	Group 2 (HMGB-1)	Group 3 (HMGB-1 + ODSH)
Total cells, $\times 10^4/\text{ml}$	7.6 \pm 1.8	21.1 \pm 3.8	13.2 \pm 2.9*
PMNs, $\times 10^4/\text{ml}$	4.0 \pm 0.8	12.0 \pm 0.8	10.2 \pm 0.6*
Total protein, $\mu\text{g}/\text{ml}$	527.3 \pm 99.7	1,645.0 \pm 689.1	1,682.1 \pm 908.7
Bronchoalveolar lavage TNF- α , pg/ml	5.9 \pm 6.8	100.4 \pm 50.7	24.1 \pm 19.0*

Data are means \pm SE. HMGB-1, high mobility group box protein-1. * P \leq 0.05 vs. group 2.

ODSH reduces airway inflammation in mice from intratracheal HMGB-1. Intratracheal HMGB-1 has been previously shown to produce a prompt influx of PMNs into the airway within 24 h (37). To determine if ODSH can also functionally block this RAGE-ligand interaction, we repeated these previously reported studies. Table 3 shows that HMGB-1 significantly increased total cells, PMNs, total protein, and TNF- α concentration in mouse bronchoalveolar lavage fluid 24 h after intratracheal instillation. Simultaneous intratracheal instillation of ODSH with HMGB-1 decreased total cells, PMNs, and TNF- α concentration, indicating that low anticoagulant ODSH can also inhibit proinflammatory RAGE-ligand interactions in vivo.

ODSH infusion can produce predictable anti-inflammatory drug concentrations in humans without anticoagulation. No serious adverse events occurred during administration of ODSH to human volunteers, and no subject experienced a decrease in circulating blood platelet concentration (see Supplemental Table 1). Bolus administration of ODSH produced dose-related increases in plasma ODSH concentrations that peaked shortly after the end of infusion and then declined in a monoexponential manner (Supplemental Fig. 2A), with peak concentrations ranging from 121 \pm 29 $\mu\text{g}/\text{ml}$ after 4 mg/kg to 359 \pm 40 $\mu\text{g}/\text{ml}$ after 20 mg/kg. Pharmacokinetic parameters from bolus ODSH administration (Supplemental Table 2) are similar to those known for unfractionated heparin. Mean clearance of ODSH was consistent through the dose range studied (10.3 to 15.4 $\text{ml}\cdot\text{h}^{-1}\cdot\text{kg}^{-1}$), and elimination half-life values were short, ranging from 1.93 to 2.72 h. Escalating doses of ODSH produced a dose-related increase in aPTT (Supplemental Fig. 2B). While the mean aPTT in subjects receiving 20 mg/kg ODSH peaked at an absolute value of 182 \pm 2 s at 40

Fig. 10. ODSH inhibits melanoma lung metastasis. Female C57BL/6J mice ($n = 6$ per group) were injected subcutaneously with 100 μl PBS, 30 mg/kg heparin, or 30 mg/kg ODSH. Thirty minutes later, 5×10^5 B16F10 melanoma cells were injected intravenously into the lateral tail vein. Twenty-seven days later, surviving mice were euthanized, lungs were removed and fixed, and visible tumor foci were counted independently by 2 different laboratory personnel blinded with regard to treatment groups. A: treatment with heparin (* P < 0.05 vs. PBS) or ODSH (** P < 0.01 vs. PBS) significantly reduced numbers of lung metastatic nodules. B: corresponding histologic sections to experiments performed in A. Compared with normal lung tissue section (B1), histology demonstrates that emergent lung metastases grow infiltratively with venous invasion and massive induction of angiogenesis in the PBS-treated group (B2). Subcutaneous heparin showed little effect on the extent of lung metastatic outgrowth (B3), but ODSH treatment suppressed lung metastatic colonization (B4). C: survival in melanoma-injected mice. ODSH treatment significantly improved 28-day survival, compared with the PBS-treated group (* P < 0.05).



min after the start of drug administration, the aPTT in two subjects receiving 80 U/kg (~ 0.5 mg/kg) of unfractionated heparin was too high (>500 s) to be accurately measured after the second blood sampling at 18 min and did not return to a measurable level (180 s) until 60 min after initial heparin administration.

The second phase I study, bolus followed by continuous 12-h infusion of ODSH, produced predictable dose- and infusion-rate related increases in both plasma concentrations of ODSH and in aPTT with ODSH concentrations reaching as high as 272 ± 61 $\mu\text{g/ml}$ when measured 12 h after bolus administration of 16 mg/kg followed by infusion of $24 \text{ mg}\cdot\text{kg}^{-1}\cdot 12 \text{ h}^{-1}$. Pharmacokinetic parameters calculated based on blood sampling after the end of drug infusion (Supplemental Table 3) were similar to those obtained from bolus administration alone, suggesting that the pharmacokinetics of ODSH elimination is linear. Clearance ranged from 9.3 to 10.8 $\text{ml}\cdot\text{h}^{-1}\cdot\text{kg}^{-1}$, and elimination half-life ranged from 1.6 to 3.6 h (Supplemental Table 3). With unfractionated heparin, therapeutic anticoagulation is usually achieved with a bolus of 80 U/kg (0.5 mg/kg) followed by an initial infusion of 18 $\text{U}\cdot\text{kg}^{-1}\cdot\text{h}^{-1}$ ($0.12 \text{ mg}\cdot\text{kg}^{-1}\cdot\text{h}^{-1}$). Supplemental Figure 2C displays mean ODSH concentrations and Supplemental Fig. 10D displays values for aPTT and PT in subjects receiving a bolus of 8 mg/kg followed by continuous infusion of $24 \text{ mg}\cdot\text{kg}^{-1}\cdot 12 \text{ h}^{-1}$ or $2 \text{ mg}\cdot\text{kg}^{-1}\cdot\text{h}^{-1}$. This dose produced peak and sustained ODSH concentrations ~ 200 $\mu\text{g/ml}$ and prolonged the aPTT from 40 to 50 s above baseline, values that represent therapeutic clinical anticoagulation. Thus the full dose of ODSH required for therapeutic anticoagulation is ~ 16 -fold higher than the anticoagulation dose of unfractionated heparin.

The third phase I safety study, in which normal volunteers received a bolus followed by drug infusion for 72 h, required drug infusion to be adjusted upward from $0.58 \text{ mg}\cdot\text{kg}^{-1}\cdot\text{h}^{-1}$ to maintain aPTT between 40–45 s. As a consequence, study subjects received between 0.64 and $1.39 \text{ mg}\cdot\text{kg}^{-1}\cdot\text{h}^{-1}$. ODSH administration in this group produced peak levels of ~ 150 $\mu\text{g/ml}$ and sustained levels ranging between 30 and 60 $\mu\text{g/ml}$ during continuous infusion (Fig. 11A), with average values for aPTT of ~ 45 s (Fig. 11B). Pharmacokinetic parameters calculated based on blood sampling after the end of drug infusion demonstrated that mean clearance was $10.25 \text{ mg}\cdot\text{h}^{-1}\cdot\text{kg}^{-1}$ and elimination half-life was 3.3 h with a range of 1.9 to 4.4 h (Supplemental Table 4). Figure 11C illustrates the relationship between ODSH plasma concentration and prolongation of aPTT. The effect of ODSH on aPTT was curvilinear and concentration dependent. Figure 11 illustrates that anti-inflammatory IC_{50} blood concentrations of ODSH can be achieved before anticoagulation is produced by this modified heparin.

Fig. 11. ODSH infusion into human volunteers achieves anti-inflammatory concentrations of drug before producing anticoagulation. ODSH was administered as a bolus (8 mg/kg) followed by continuous intravenous infusion of 0.64 to $1.39 \text{ mg}\cdot\text{kg}^{-1}\cdot\text{h}^{-1}$ ODSH to normal volunteers. *A*: mean plasma levels of ODSH during study drug infusion. *B*: change (means \pm SD) in activated partial thromboplastin time (aPTT) and partial thromboplastin (PT) during study drug infusion. *C*: relationship is shown between plasma ODSH and change in aPTT from baseline during 3-day infusion of 8 mg/kg followed by $0.5 \text{ mg}\cdot\text{kg}^{-1}\cdot\text{h}^{-1}$ adjusted to maintain an aPTT between 40 and 45 s. Anti-inflammatory IC_{50} concentrations of ODSH are achieved before any substantial anticoagulant effect on aPTT.

DISCUSSION

Heparin has long been recognized not only for its anticoagulant effects but also for its anti-inflammatory pharmacology. Using a selective ODSH with low anticoagulant potency, we have confirmed that heparin possesses a number of previously recognized anti-inflammatory activities that are independent of ATIII binding and other anticoagulant activities. ODSH possesses low binding affinity for ATIII (Fig. 1) and low anti-Xa and anti-IIa anticoagulant activities and inhibits complement activation (14), P-selectin-mediated cellular adhesion (Fig. 5), and proteolytic activities of the cationic leukocyte proteases HLE and cathepsin G (Fig. 8, A and B; Table 2), as reported for heparin (14, 45, 46). In this investigation, we extend the understanding of heparin's nonanticoagulant pharmacology by showing that heparin and low anticoagulant ODSH prevent inflammatory cells from utilizing RAGE as a vascular adhesion molecule (Fig. 6; Table 1) and interfere with the binding of azurocidin (Fig. 7), the enzymatically inactive HLE homologue that enhances vascular permeability following leukocyte adherence to the microvessel wall (15). Perhaps just as important for its overall anti-inflammatory activities, ODSH and heparin both inhibit the interaction of RAGE with the AGE product CML-BSA (Fig. 9A), the nuclear alarmin HMGB-1 (Fig. 9B), and the calgranulin S100b (Fig. 9C). Inhibition of ligand binding to receptors was also functionally important. ODSH significantly reduced selectin-mediated lung metastasis of B16 melanoma cells (Fig. 10) and inhibited airway inflammation from intratracheal HMGB-1 (Table 3) in mice. Surprisingly, ODSH retains many of the activities of heparin, confirming that the anti-inflammatory activities of heparin are not dependent upon anticoagulation. Disruption of ATIII binding by 2-O and 3-O desulfation also increases the margin of safety as a pharmacologic agent compared with parent heparin. Unlike heparin, ODSH has no propensity to activate factor XII (Fig. 3). Furthermore, ODSH does not trigger platelet activation in the HIT SRA (Fig. 2A) and even suppresses serotonin release

that is stimulated by low concentrations of heparin (Fig. 2B). Blood concentrations of ODSH that are severalfold higher than those required for anti-inflammatory activities could be achieved and maintained in human volunteers without excessive anticoagulation (Fig. 11). Thus selectively desulfated heparin can function safely as an anti-inflammatory molecule that disrupts at many of the sequential events in leukocyte-mediated inflammation (Fig. 12): tethering and rolling (selectin inhibition), arrest (Mac-1/RAGE inhibition), diapedesis (azurocidin inhibition), and secretion of proinflammatory granular contents into the external milieu (inhibition of HLE, cathepsin G, azurocidin, and S100 calgraulin).

The anionic sulfates and carboxylates of heparin have recently been studied to assess their importance for binding of the polysaccharide to proteins. Whereas the 6-O sulfate of glucosamine is essential for heparin binding to P- and L-selectins (45), the 2-O sulfate is important for heparin binding to many fibroblast growth factors (2). From our studies, it is apparent that the 2-O sulfate of α -L-iduronic acid can be removed without impairing the ability of heparin to inhibit complement, P-selectin, PMN proteases, or azurocidin, and with only modest decreases in the activity for inhibiting RAGE-ligand interactions. More importantly, 2-O sulfation of α -L-iduronic acids appears essential for the interaction of heparin and PF4, with subsequent binding of the antibody that produces platelet activation in the HIT syndrome, resulting in substantially increased risk of disastrous venous and arterial thromboembolism in as many as 3–5% of individuals who receive heparin therapy (44). Surprisingly, ODSH consistently suppressed heparin-induced serotonin release when present in concentrations of $\geq 25 \mu\text{g/ml}$ (Fig. 2B). The mechanism of this suppression is not apparent for our studies but is consistent with the observation that higher concentrations of heparin above those appropriate for therapeutic anticoagulation can inhibit SRA reactions by skewing the glycosaminoglycans-to-PF4 ratio out of the optimal range required for formation of

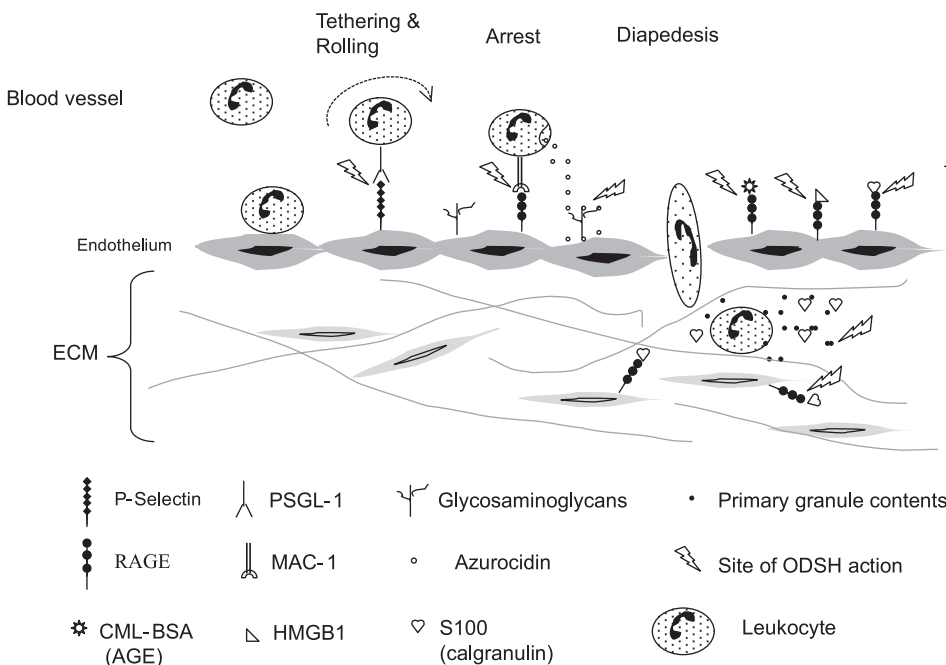


Fig. 12. Anti-inflammatory effects of heparin and low anticoagulant ODSH. Recruitment of leukocytes to the injured or inflamed tissue is a multistep process involving interaction of leukocyte ligands with endothelial adhesion molecules. Heparin and ODSH 1) inhibit tethering and rolling of leukocytes on the endothelial surface through leukocyte ligand and PSGL-1 binding to endothelial P-selectin, 2) inhibit firm attachment of leukocyte through Mac-1 interaction with endothelial RAGE, 3) prevent diapedesis of leukocytes by protecting endothelial barrier function through binding to azurocidin, 4) prevent tissue destruction by inhibiting the leukocyte granule proteases, and 5) prevent sustained inflammatory signaling by RAGE by inhibiting fluid phase RAGE ligand (CML-BSA, HMGB1, and S100/calgranulin) interaction with endothelial and mesenchymal cell surface RAGE.

HIT antigenic complexes on the platelet surface (35). The heparin-induced SRA was suppressed by ODSH concentrations (25 $\mu\text{g/ml}$) that are well below those that cause anticoagulation in animals or humans (Fig. 11), suggesting that ODSH might be considered as a treatment for HIT. This supposition is supported by the finding that circulating platelet counts have not fallen significantly in >100 human subjects who have thus far received prolonged infusion ODSH during clinical trials (data on file at FDA and with ParinGenix). Taken together, these observations suggest that removal of 2-*O* sulfates can considerably improve the clinical safety of heparin without substantially harming its anti-inflammatory efficacy.

A major finding of this investigation is that both heparin and low anticoagulant ODSH have broad activity to inhibit ligand binding to RAGE. RAGE is composed of three immunoglobulin-like regions: a distal "V" type domain, followed by two "C" type domains, a short transmembrane domain and a cytoplasmic tail required for signaling. Rather than being specific for a single ligand, RAGE is a pattern recognition receptor that will bind a number of other ligands (40), including HMGB-1, S100/calgranulins, Alzheimer's A β peptide, and amyloid A. Once ligated and activated, RAGE mediates postreceptor signaling including activation of NF- κ B, leading to a profound inflammatory response (40). Through the influence of a prominent NF- κ B-responsive consensus sequence in its promoter, activation of RAGE also leads to even greater RAGE expression (40). RAGE interacts with the leukocyte β_2 -integrins Mac-1 (CD11b/CD18) and p150,95 (CD11c/CD18) to facilitate phagocytic inflammatory cell recruitment (8). The attraction of leukocytes to areas of inflammation is further augmented by interaction of the RAGE ligands S100/calgranulins (8) and HMGB-1 (31). Thus RAGE can mediate a vicious cycle of sustained, smoldering inflammation. Experimentally, RAGE-mediated inflammation has been inhibited in animal models of diabetes or inflammation by daily injections of recombinant sRAGE (soluble RAGE composed of the ligand binding domains but lacking transmembrane or cytoplasmic domains; Ref. 16). While sRAGE is effective at inhibiting RAGE in animal models, it is a recombinant protein that will be relatively expensive for human disease and possibly immunogenic with long-term use. Thus our observation that low anticoagulant heparin can prevent RAGE-ligand interactions is potentially important as a more practical therapeutic strategy for RAGE inhibition in humans.

The extracellular domain of RAGE has been recently engineered and used in detailed analyses of RAGE-ligand interactions in vitro (12, 23, 26, 49, 50). Studies (12) suggest that the V and C1 extracellular domains form an integrated structural binding unit, with C2 functioning independently through attachment to VC1 by a flexible linker. Whereas AGEs and amphoterin bind to the V domain (50), the calgranulin S100A12 binds to the C1 domain (49), S100b binds to both V and C1 domains (12), and S100A6 binds to V and C2 (23). Heparin inhibits many proteins through electrostatic charge interactions with cationic amino acids (14, 43). Evidence suggests that electrostatic charge interactions may also play an important role in ligand-RAGE binding. AGEs are negatively charged as the result of the Maillard formation reaction, by which reducing sugars or aldehydes modify arginines and lysines to produce glycosylated proteins, adding a net negative charge on the proteins at physiologic pH (48). The AGE

binding region of the V domain consists of a large hydrophobic cavity rimmed on its surface with basic amino acids to form a cationic center (50). AGE binding to the V region of RAGE is initially facilitated by the ionic attraction between the positive charges of RAGE and the negative charges of AGE. The binding complex is then stabilized with hydrophobic interaction after conformational changes (48). Heparin and nonanticoagulant heparins such as ODSH might be expected to disrupt these interactions by competing with AGEs for binding to the cationic V region. Because heparin and ODSH are large, long polymers, their electrostatic attachment to the V domain of RAGE might also cause steric hindrance for S100/calgranulin binding to adjacent C1 and C2 domains. In this manner, heparin and ODSH might inhibit RAGE binding to S100 calgranulins that primarily interact with C1 and C2 as opposed to the V domain. The importance of charge for inhibition of RAGE-ligand binding is underscored by the fact that the modest desulfation present in ODSH also modestly reduces the potency of the polysaccharide for inhibiting RAGE-ligand interactions (Figs. 6 and 9; Table 1).

In the almost 100 yr since its discovery, heparin continues to be used primarily as an anticoagulant for prevention or treatment of thrombosis. With the recent emergence of intravenously active direct thrombin inhibitors and orally bioavailable small molecule inhibitors of factor Xa, both of which are free of the risk of HIT, heparin's life as an anticoagulant may be clinically nearing an end. However, the realization that low anticoagulant heparins such as ODSH are free of HIT reactivity and retain unfractionated heparin's broad and redundant range as an anti-inflammatory agent, including inhibition of RAGE-ligand interactions, may endow this old and well-understood drug with a new and important use in the treatment of human diseases.

GRANTS

This work was supported by a sponsored research project awarded to the University of Utah by ParinGenix (to N. V. Rao).

DISCLOSURES

Dr. T. P. Kennedy is the inventor of US Patents 5,707,974; 5,912,237; 5,990,097; 6,024,940; 6,077,683; 6,489,311; and 7,468,358, all related to OSDH and owned by ParinGenix, (Weston, FL). Dr. T. P. Kennedy owns founder's stock in ParinGenix.

REFERENCES

- Altinbas M, Coskun HS, Er O, Ozkan M, Eser B, Unal A, Cetin M, Soyuer S. A randomized clinical trial of combination chemotherapy with and without low-molecular-weight heparin in small cell lung cancer. *J Thromb Haemost* 2: 1266–1261, 2004.
- Ashikari-Hada S, Habuchi H, Kariya Y, Itoh N, Reddi AH, Kimata K. Characterization of growth factor-binding structures in heparin/heparan sulfate using an octasaccharide library. *J Biol Chem* 279: 12346–12354, 2004.
- Ashikari-Hada S, Habuchi H, Kariya Y, Kimata K. Heparin regulates vascular endothelial growth factor₁₆₅-dependent mitogenic activity, tube formation, and its receptor phosphorylation of human endothelial cells. Comparison of the effects of heparin and modified heparins. *J Biol Chem* 280: 31508–31515, 2005.
- Barker RL, Gundel RH, Gleich GJ, Checkel JL, Loegering DA, Pease LR, Hamann KJ. Acidic polyamino acids inhibit human eosinophil granule major basic protein toxicity. Evidence of a functional role for ProMBP. *J Clin Invest* 88: 798–805, 1991.
- Borsig L, Wong R, Feramisco J, Nadeau DR, Varki NM, Varki A. Heparin and cancer revisited: mechanistic connections involving platelets,

- P-selectin, carcinoma mucins, and tumor metastasis. *Proc Natl Acad Sci USA* 98: 3352–3357, 2001.
6. Borsig L, Wong R, Hynes RO, Varki NM, Varki A. Synergistic effects of L- and P-selectin in facilitating tumor metastasis can involve non-mucin ligands and implicate leukocytes as enhancers of metastasis. *Proc Natl Acad Sci USA* 99: 2193–2198, 2002.
 7. Cardin A, Weintraub H. Molecular modeling of protein-glycosaminoglycan interactions. *Arteriosclerosis* 9: 21–32, 1989.
 8. Chavakis T, Bierhaus A, Al-Fakhri N, Schneider D, Witte S, Linn T, Nagashima M, Morser J, Arnold B, Preissner KT, Nawroth PP. The pattern recognition receptor (RAGE) is a counterreceptor for leukocyte integrins: a novel pathway for inflammatory cell recruitment. *J Exp Med* 198: 1507–1515, 2003.
 9. Cheng Y, Prusoff W. Relationship between the inhibition constant (K_i) and the concentration of inhibitor which causes 50 per cent inhibition (IC₅₀) of an enzymatic reaction. *Biochem Pharmacol* 22: 3099–3108, 1973.
 10. Dudas B, Rose M, Cornelli U, Pavlovich A, Hanin I. Neuroprotective properties of glycosaminoglycans: potential treatment for neurodegenerative disorders. *Neurodegener Dis* 5: 200–205, 2008.
 11. Diamond M, Alon R, Parkos C, Quinn M, Springer T. Heparin is an adhesive ligand for the leukocyte integrin Mac-1 (CD11b/CD1). *J Cell Biol* 130: 1473–1482, 1995.
 12. Dattilo BM, Fritz G, Leclerc E, Kooi CW, Heizmann CW, Chazin WJ. The extracellular region of the receptor for advanced glycation end products is composed of two independent structural units. *Biochemistry* 46: 6957–6970, 2007.
 13. Fryer AD, Jacoby DB. Function of pulmonary M₂ muscarinic receptors in antigen-challenged guinea pigs is restored by heparin and poly-L-glutamate. *J Clin Invest* 90: 2292–2298, 1992.
 14. Fryer A, Huang YC, Rao G, Jacoby D, Mancilla E, Whorton R, Piantadosi CA, Kennedy T, Hoidal J. Selective O-desulfation produces nonanticoagulant heparin that retains pharmacologic activity in the lung. *J Pharmacol Exp Ther* 282: 208–219, 1997.
 15. Gautam N, Olofsson A, Herwald H, Iversen L, Lundgren-Akerlund E, Hedqvist P, Arfors KE, Glodgaard H, Lindbom L. Heparin-binding protein (HBP/CAP37): a missing link in neutrophil-evoked alteration of vascular permeability. *Nat Med* 2: 1123–1127, 2001.
 16. Goldin A, Beckman JA, Schmidt AM, Creager MA. Advanced glycation end products. Sparking the development of diabetic vascular injury. *Circulation* 114: 597–605, 2006.
 17. Hanford LE, Enghild JJ, Valnickova Z, Petersen SV, Schaefer LM, Schaefer TM, Reinhart TA, Oury TD. Purification and characterization of mouse soluble receptor for advanced glycation end products (sRAGE). *J Biol Chem* 279: 50019–50024, 2004.
 18. Hofmann MA, Drury S, Fu C, Qu W, Taguchi A, Lu Y, Avila C, Kambham N, Bierhaus A, Nawroth P, Neurath MG, Slattery T, Beach D, McClary J, Nagahima M, Morser J, Stern D, Schmidt AM. RAGE mediates a novel proinflammatory axis: a central cell surface receptor for S100/calgranulin polypeptides. *Cell* 97: 889–901, 1999.
 19. Hori O, Brett J, Slattery T, Cao R, Zhang J, Chen J, Nagashima M, Lundh ER, Vijay S, Nitecki D, Morser J, Stern D, Schmidt AM. The receptor for advanced glycation end products (RAGE) is a cellular binding site for amphotericin. Mediation of neurite outgrowth and co-expression of rAge and amphotericin in the developing nervous system. *J Biol Chem* 270: 25752–25761, 1995.
 20. Kakkar AK, Levine MN, Kadziola Z, Lemoine NR, Low V, Patel HK, Rustin G, Thomas M, Quigley M, Williamson RCH. Low molecular weight heparin, therapy with dalteparin, and survival in advanced cancer: The Fragmin Advanced Malignancy Outcome Study (FAMOUS). *J Clin Oncol* 22: 1944–1948, 2004.
 21. Klerk CP, Smorenburg SM, Otten HM, Lensing AW, Prins MH, Piovella F, Prandoni P, Bos MM, Richel DJ, van Tienhoven G, Buuler HR. The effect of low molecular weight heparin on survival in patients with advanced malignancy. *J Clin Oncol* 23: 21230–2135, 2005.
 22. Koenig A, Norgard-Sumnicht K, Linhardt R, Varki A. Differential interactions of heparin and heparan sulfate glycosaminoglycans with the selectins. Implications for the use of unfractionated and low molecular weight heparins as therapeutic agents. *J Clin Invest* 101: 877–889, 1998.
 23. Leclerc E, Fritz G, Weibel M, Heizmann CW, Galichet A. S100B and S100A6 differentially modulate cell survival by interacting with distinct RAGE (receptor for advanced glycation end products) immunoglobulin domains. *J Biol Chem* 282: 31317–31331, 2006.
 24. Lee AYY, Rickles FR, Julian JA, Gent M, Baker RI, Bowden C, Kakkar AK, Prins M, Levine NM. Randomized comparison of low molecular weight heparin and coumarin derivatives on the survival of patients with cancer and venous thromboembolism. *J Clin Oncol* 23: 2123–2129, 2005.
 25. Lever R, Page CP. Novel drug development opportunities for heparin. *Nat Rev Drug Disc* 1: 140–148, 2002.
 26. Matsumoto S, Yoshida T, Murata H, Harada S, Fujita N, Nakamura S, Yamamoto Y, Watanabe T, Yonekura H, Yamamoto H, Ohkubo T, Kobayashi Y. Solution structure of the variable-type domain of the receptor for advanced glycation end products: new insight into AGE-RAGE interaction. *Biochemistry* 47: 12299–12311, 2008.
 27. McClean J. The thromboplastic action of cephalin. *Am J Physiol* 41: 250–257, 1916.
 28. McEver R, Cummings R. Role of PSGL-1 binding to selectins in leukocyte recruitment. *J Clin Invest* 100: S97–103, 1997.
 29. Myint KM, Yamamoto Y, Doi T, Kato I, Harashima A, Yonekura H, Watanabe T, Shinohara H, Takeuchi M, Tsuneyama K, Hashimoto N, Asano M, Takasawa S, Okamoto H, Yamamoto H. RAGE control of diabetic nephropathy in a mouse model. Effects of RAGE gene disruption and administration of low-molecular weight heparin. *Diabetes* 55: 2510–2522, 2006.
 30. Ono K, Hattori H, Takeshita S, Kurita A, Ishihara M. Structural features in heparin that interact with VEGF₁₆₅ and modulate its biological activity. *Glycobiology* 9: 705–711, 1999.
 31. Orlova VV, Choi EY, Xie C, Chavakis E, Bierhaus A, Ihanus E, Ballantyne CM, Gahmberg CG, Bianchi ME, Nawroth PP, Chavakis T. A novel pathway way of HMGB1-mediated inflammatory cell recruitment that requires Mac-1 integrin. *EMBO J* 26: 1129–1139, 2007.
 32. Patey SJ, Edwards EA, Yates EA, Turnbull JE. Heparin derivatives as inhibitors of BACE-1, the Alzheimer's beta-secretase, with reduced activity against factor Xa and other proteases. *J Med Chem* 49: 6129–6132, 2006.
 33. Pham C. Neutrophil serine proteases: specific regulators of inflammation. *Nat Rev Immunol* 6: 541–550, 2006.
 34. Prechel MM, McDonald MK, Jeske WP, Messmore HL, Walenga JM. Activation of platelets by heparin-induced thrombocytopenia antibodies in the serotonin release assay is not dependent on the presence of heparin. *J Thromb Haemost* 3: 2168–2175, 2005.
 35. Rauova L, Zhai L, Kowalska A, Arepally GM, Cines DB, Poncz M. Role of platelet surface PF4 antigenic complexes in heparin-induced thrombocytopenia pathogenesis: diagnostic and therapeutic implications. *Blood* 107: 2346–2353, 2006.
 36. Rauvala H, Pihlaskari R. Isolation and some characteristics of an adhesive factor of brain that enhances neurite outgrowth in central neurons. *J Biol Chem* 262: 16625–16635, 1987.
 37. Rowe SM, Jackson PL, Liu G, Hardison M, Livraghi A, Solomon GM, McQuaid DB, Noerager BD, Gaggari A, Clancy JP, O'Neal W, Sorcher EJ, Abraham E, Blalock JE. Potential role of high-mobility group box 1 in cystic fibrosis airway disease. *Am J Respir Crit Care Med* 178: 822–831, 2008.
 38. Samuel M, Pixley RA, Villanueva MA, Colman RW. Human factor XII (Hageman factor) autoactivation by dextran sulfate: circular dichroism, fluorescence, and ultraviolet difference spectroscopic studies. *J Biol Chem* 267: 19691–19697, 1992.
 39. Schmidt AM, Vianna M, Gerlach M, Brett J, Ryan J, Kao J, Esposito C, Hegarty H, Hurley W, Clauss M, Wang F, Peng YCE, Tsang TC, Stern D. Isolation and characterization of two binding proteins for advanced glycosylation end products from bovine lung which are present on the endothelial cell surface. *J Biol Chem* 267: 14987–14997, 1992.
 40. Schmidt AM, Yan SD, Yan SF, Stern DM. The multiligand receptor RAGE as a progression factor amplifying immune and inflammatory responses. *J Clin Invest* 108: 949–955, 2001.
 41. Silverberg M, Dunn JT, Garen L, Kaplan AP. Autoactivation of human Hageman factor. Demonstration using a synthetic substrate. *J Biol Chem* 255: 7281–7286, 1980.
 42. Stevenson JL, Choi SH, Varki A. Differential metastasis inhibition by clinically relevant levels of heparins—correlation with selectin inhibition, not antithrombotic activity. *Clin Cancer Res* 11: 7003–7011, 2005.
 43. Thourani VH, Brarr SS, Kennedy TP, Thornton LR, Watts JA, Ronson RS, Zhao ZQ, Sturrock AL, Hoidal JR, Vinten-Johansen J. Nonanticoagulant heparin inhibits NF-κB activation and attenuates myo-

- cardial reperfusion injury. *Am J Physiol Heart Circ Physiol* 278: H2084–H2093, 2000.
44. **Walenga JM, Jeske WP, Prechel MM, Makhos M.** Newer insights on the mechanism of heparin-induced thrombocytopenia. *Semin Thromb Hemost* 30, Suppl 1: 57–67, 2004.
 45. **Wang L, Brown JR, Varki A, Esko JD.** Heparin's anti-inflammatory effects require glucosamine 6-O-sulfation and are mediated by blockade of L- and P-selectins. *J Clin Invest* 110: 127–136, 2001.
 46. **Weiler JM, Edens RE, Linhardt RJ, Kapelanski DP.** Heparin and modified heparin inhibit complement activation in vivo. *J Immunol* 148: 3210–3215, 1992.
 47. **Weiss S.** Tissue destruction by neutrophils. *N Engl J Med* 320: 365–376, 1989.
 48. **Westwood ME, Thornally PJ.** Molecular characteristics of methylglyoxal-modified bovine and human serum albumins. Comparison with glucose-derived advanced glycation endproduct-modified serum albumins. *J Protein Chem* 14: 359–372, 1995.
 49. **Xie J, Burz DS, He W, Bronstein IB, Lednev I, Shekhtman A.** Hexameric calgranulin C (S100A12) binds to the receptor for advanced glycated end products (RAGE) using symmetric hydrophobic target-binding patches. *J Biol Chem* 282: 4218–4231, 2007.
 50. **Xie J, Reverdatto S, Frolov A, Hoffmann R, Burz DS, Shekhtman A.** Structural basis for pattern recognition by the receptor for advanced glycation end products (RAGE). *J Biol Chem* 282: 27255–27269, 2008.

